

Maintaining Electrochemical Performance of Flexible ITO-PET Electrodes under High Strain

Laura J. Waldman, Daniel P. Haunert, Jack D. Carson, Nate Weiskopf, Julia V. Waldman, and Gabriel LeBlanc*



Cite This: *ACS Omega* 2024, 9, 29732–29738



Read Online

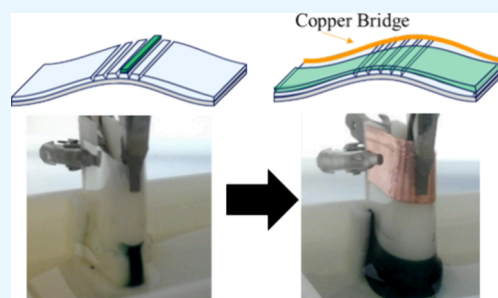
ACCESS |

Metrics & More

Article Recommendations

Supporting Information

ABSTRACT: Flexible electrode materials, particularly indium tin oxide (ITO)-coated polyethylene terephthalate (PET), have attracted the attention of researchers for a wide variety of applications. However, there has been limited attention to the effects of electrode flexibility during electrochemical processes. In this research article, we studied how bending commercially available ITO-PET electrodes impacts the electrodeposition process of polyaniline (PANI). Thicker ITO layers start cracking at a normalized strain of 0.10 (bending radius of 10 mm), and cracking becomes detrimental to full deposition at a normalized strain of 0.16 or higher (bending radius of 6 mm or lower). Thinner ITO layers were evaluated as electrodes in electrochemical applications; however, the higher resistance of these electrodes prevented uniform electrodeposition of PANI. In order to overcome the issues of cracking, conductive thin films and copper tape were explored as low-cost methods for electrically bridging cracks in the electrode. While conductive thin films reduced the resistance effect, copper tape was found to fully restore the original electrochemical activity as measured by chronoamperometry and enable uniform electrodeposition at a bending radius as low as 3 mm. This strategy was then demonstrated by performing electrochromic bleaching of PANI under high-strain conditions. These studies illustrate some of the limitations of ITO-PET electrodes and strategies for overcoming these limitations for future applications that require a high degree of flexibility in a transparent electrode substrate.



INTRODUCTION

Transparent conducting oxides, especially indium tin oxide (ITO), have been extensively used as electrodes in applications that require transparency in the visible region of the electromagnetic spectrum. These applications range from touch screen panels¹ to solar cells² and have become integral to many popular technologies used today. While ITO is typically deposited onto rigid substrates such as glass, ITO-coated plastics (such as polyethylene terephthalate (PET)) are also commercially available. These ITO plastics are typically less conductive than ITO on rigid surfaces (e.g., glass) but provide alternative benefits including flexibility and reduced weight and cost of the electrode, opening opportunities for these electrodes to be used in new areas.³ While these electrodes are commonly employed in electrochemical studies, their performance is rarely evaluated in conditions requiring flexibility. The challenge of performing electrochemical experiments under strained or bent conditions has contributed to the limited understanding of the interplay between flexibility and electrochemical performance.

The thickness and doping level of the ITO have a major impact on the properties of transparent electrodes. It is well established that there is a tradeoff in optical transparency and conductivity, with thicker ITO layers and higher doping levels increasing conductivity but decreasing transparency.⁴ When

ITO is deposited on a flexible substrate, such as PET, the relationship between ITO thickness and flexibility also becomes important as ITO is a ceramic material and therefore brittle. Previous studies have demonstrated that bending ITO-PET electrodes beyond a certain threshold strain results in cracks in the ITO layer and dramatically increases the resistance of the electrode.^{5,6} As expected, the strain that the ITO electrode could withstand before significant changes in resistance was related to the ITO layer thickness. Thinner ITO layers can achieve a tighter bending radius before cracking decreases the performance. More recently, the importance of flexibility has led researchers to develop ITO layers with thicknesses less than 25 nm.^{7,8} Such electrodes maintain their electrical properties at bending radii as low as 2 mm, though the sheet resistance of these electrodes is still in the hundreds or thousands of Ω/\square . While such high resistances are suitable for many electrical applications (e.g., touchscreens), electrochemical processes are likely to be hindered.

Received: April 5, 2024

Revised: June 4, 2024

Accepted: June 13, 2024

Published: June 24, 2024



Nevertheless, the advantages of using flexible ITO electrodes in electrochemical applications have encouraged their development over the past few decades. In one early example published in 2003, Mitsubayashi et al fabricated an ITO-PET-based glucose sensor.⁹ More recent examples include the development of sensors for heavy metals,¹⁰ biofilms,¹¹ pH,¹² neurotransmitters,¹³ and DNA hybridization.¹⁴ In addition to sensors, flexible ITO electrodes have been used as substrates for the electrodeposition of active materials including metal oxides,¹⁵ nanomaterials,¹⁶ and conductive polymers^{12,17–19} with applications including piezoelectrics,²⁰ electrochromic devices,²¹ and supercapacitors^{22,23} to name just a few. However, in these examples, the ITO layer thickness is generally quite high (>100 nm), and the analysis of flexibility is typically limited to a picture of the device performance in a mild bending configuration, if included at all.

Understanding the flexibility limits of ITO-PET electrodes for electrochemical applications is important for their practical deployment. This was highlighted in a recent communication from our research group that showed how the electrochemical deposition of polyaniline (PANI) and subsequent electrochemical behavior significantly changed below a bending radius of 7.5 mm.²⁴ In the current study, we electrodeposited PANI onto commercially available ITO-PET substrates to elucidate the relationship between strain and electrochemical performance. 3D-printed electrochemical cells allow for the evaluation of these electrodes under a wide range of bending radii. PANI was chosen as a test material for evaluating the effects of strained electrochemical conditions because it is easily deposited and visualized on ITO. Additionally, the conductive nature of PANI and its variety of applications make it an interesting material to study on ITO substrates. Beyond simple evaluation, this study also looked to overcome limitations associated with the flexibility of these devices in electrochemical settings by using conductive polymers and conductive tape to enable the use of this commercially available electrode under high-strain conditions.

RESULTS AND DISCUSSION

ITO-PET is commercially available at a wide range of surface resistivity, which can be controlled by either changing the ITO layer thickness or the dopant concentration of the ITO. In this study, we employed ITO-PET commercially available from Sigma Aldrich, which sells ITO with surface resistivity ranging from 60 to 300 Ω/\square (Supporting Information Table S1). Typically, the additional thickness of the ITO required to achieve higher electrical conductivity reduces the optical transparency of the ITO film. Applications requiring higher optical transparency may use an electrode with higher resistivity. Additionally, previous studies have shown that the thickness of the ITO layer can play a critical role in the practical flexibility of the electrode, with flexibility moderately improved in electrodes with thinner ITO layers.^{6–8} Because these thinner electrodes have higher electrical resistance, it is critical that the higher resistance does not limit the electrochemical performance of the electrode.

To evaluate the electrochemical performance of these electrodes, electrodeposition of PANI was performed on ITO samples with different resistivity values using unstrained (flat) conditions. PANI only successfully deposited on films with 60 Ω/\square or 100 Ω/\square resistivity (Figure 1). Higher resistivity ITO-PET electrodes prevented the deposition of PANI (Supporting Information Figure S1). Interestingly, the

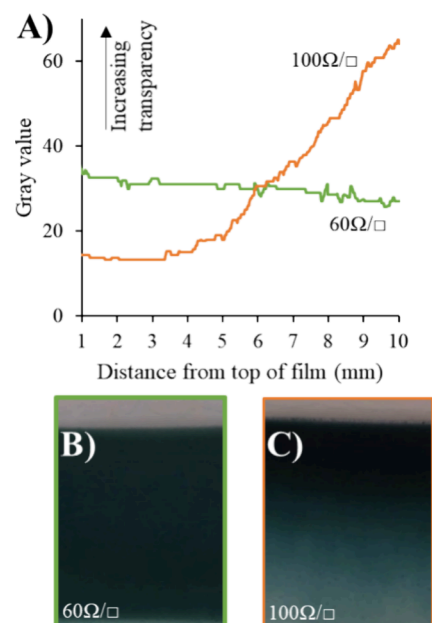


Figure 1. Effect of ITO resistance on the uniformity of PANI electrodeposition. (A) Gray value of PANI as a function of distance from the top of the electrode for a sample deposited on 60 Ω/\square (green) and 100 Ω/\square (orange). (B) Optical photograph of the PANI deposition on 60 Ω/\square ITO. (C) Optical photograph of the PANI deposition on 100 Ω/\square ITO.

deposition of PANI did not occur uniformly across the 100 Ω/\square electrode exposed to the electrolyte (Figure 1C). Instead, the deposition formed as a gradient, with a higher concentration of the PANI closer to the point of electrical connection. This is quantified using the “gray value plot profile” shown in Figure 1A, with a lower gray value indicating a darker portion of the film. At the bottom of the electrode, farther away from the electrical connection, the PANI layer was thin or incomplete. According to Ohm’s law, we should expect an effective voltage drop along the length of the electrode. This resistance effect on the current distribution is often referred to as the “terminal effect” and has been studied in different electrochemical systems including metal electrodepositions²⁵ and electrochromic windows.²⁶ As the resistance of the electrode increases, this voltage drop is expected to become more pronounced. 60 Ω/\square films appear opaque throughout the length of the film, but for the 100 Ω/\square , the opacity of the deposition decreases along the length of the electrode. For higher resistivity films, the voltage drop prevents successful deposition altogether. Unfortunately, an increase in the deposition voltage did not significantly improve the deposition of PANI on higher-resistivity ITO electrodes. The flexibility benefit gained by use of these electrodes is therefore offset by the decrease in electrochemical activity. As demonstrated by the failure of deposition in this study, thin ITO films may be unusable in certain electrochemical applications.

Electrodeposition was then performed on the most conductive (60 Ω/\square , 130 nm thick) ITO-PET substrates in 3D-printed electrochemical cells designed to hold the electrode at a specific bending radius from 12 to 3 mm. As the bending radius decreases, the strain experienced by the ITO increases. When the PET films are bent to a certain radius, the strain on the film is determined by the distance from the centerline of the film to the surface divided by the

bending radius. All electrodes used in these strained experiments have uniform thickness which is thin relative to the range of bending radii, so normalized strain ($1/\text{bending radius}$ in mm) is used in this study. The custom electrochemical cells are used to determine how flexible electrodes behave under strained conditions and the designs are freely available on the NIH print exchange (see Supporting Information). On the $60 \Omega/\square$ films, electrodepositions could be reproducibly generated down to a normalized strain of approximately 0.10 (bending radius of 10 mm) based on quantification of the film coverage using ImageJ (Figure 2). At higher strain, the

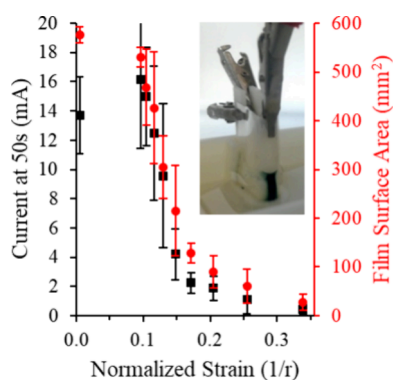


Figure 2. Deposition of PANI on ITO substrates held under different levels of strain ($1/\text{bending radius}$). Current at 50 s (left axis, black) and deposition area (right axis, red) of samples held at various levels of strain. Error bars represent the standard deviation from at least 3 unique samples. Inset is a photograph of a deposition taking place at a normalized strain of 0.33 (bending radius of 3 mm).

deposition became less consistent, and at a bending radius of 5 mm or tighter, it was limited to the central portion of the electrode, in good agreement with our previous findings.²⁴ Interestingly, at these higher strained conditions, the electro-deposition could be localized in different regions by changing the location of the electrical connection (Supporting Information Figure S2). When connected to the electrode at the center point, analysis of the current during deposition and the surface area of the deposited film as a function of the normalized strain (Figure 2) demonstrates that the smaller deposition area at a higher strain is due to lower current, suggesting that only a portion of the electrode is active under high-strain conditions. Importantly, the localized deposition differs from the “terminal effect” observed in the $100 \Omega/\square$ ITO electrodes seen in Figure 1 in two ways: localized deposition occurs perpendicularly to the direction of terminal effect deposition, and the localized deposition occurs in discrete segments rather than as a gradient. These differences indicate that the terminal effect deposition (Figure 1) and the localized deposition (Figure 2) are caused by different mechanisms.

We hypothesized that the isolated depositions occurred due to cracking in the ITO layer because ITO is known to be a brittle material. This cracking would electrically isolate segments of the electrode and cause localized electro-depositions. While cracking was not observed visibly or under a light microscope, we performed SEM analysis on ITO samples bent at various bending radii and found an increasing amount of cracking as the strain increased (Supporting Information Figure S3). As the electrode is bent to smaller radii, the strain (change in length) on the ITO layer

increases as well. Because ITO is brittle, the ITO layer cannot deform to accommodate the strain, but cracks instead. This is related to the adhesion of the film as determined by the effective interfacial shear strength.^{27,28} Importantly, the cracks occur parallel to one another and parallel to the axis of bending (Figure 3A), which explains the deposition of the PANI in a

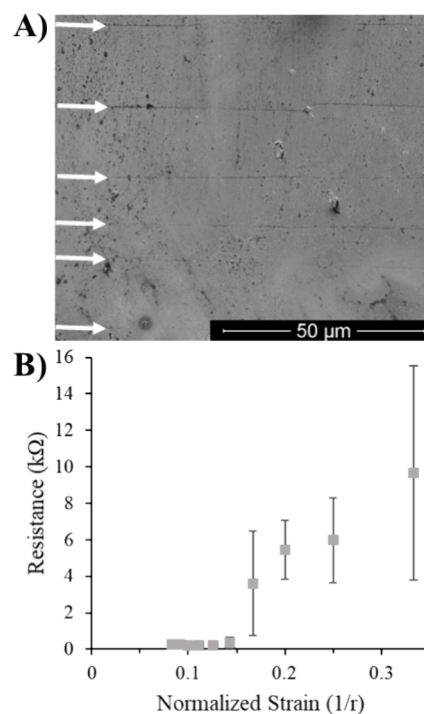


Figure 3. Effect of bending ITO electrodes. (A) SEM image of cracking in 130 nm-thick ITO layer after the sample was bent at a 3 mm bending radius. Arrows were added to highlight crack location and orientation. (B) Measured resistance of 130 nm-thick ITO layer under different levels of strain ($1/\text{bending radius}$). Error bars represent the standard deviation from at least 3 unique samples.

vertical direction in line with the electrode connection. Additionally, while the electrodes themselves showed no visible changes in appearance by the naked eye or under a light microscope, the change in resistance across the horizontal direction of the electrode could be easily observed using linear sweep voltammetry (Figure 3B). The dramatic rise in resistance at higher strain explains why the deposition became even more isolated because segments of the electrode become effectively separated. This correlation between change in resistance and change in electrochemical performance can therefore serve as a simple method for determining the limiting strain for other flexible electrochemical systems.

Because thicker ITO electrodes ($60 \Omega/\square$, 130 nm thick) appear necessary for good electrochemical activity, a method for electrically connecting the various ITO segments under strained conditions is needed for applications requiring flexibility. Two approaches were attempted in this effort to connect the ITO segments: conductive tape was applied to the point of contact of the electrode and an electrodeposited film was used to bridge the cracks in the underlying ITO electrode (Figure 4).

In the first approach, a thin strip of conductive copper tape was applied along the top of the ITO electrode. When the resistance of the electrode was measured under high-strain

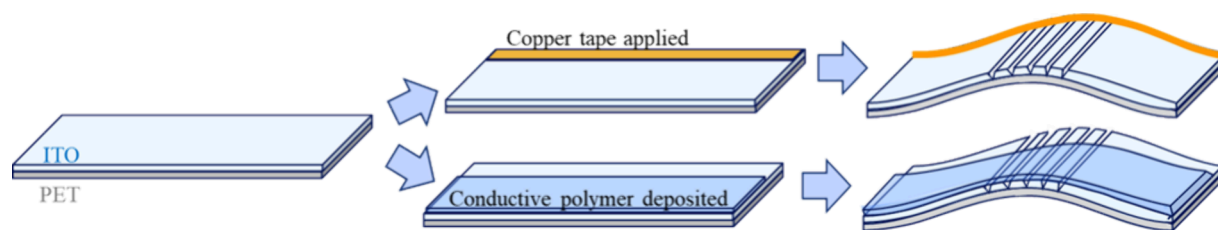


Figure 4. Illustration of the two approaches taken for bridging cracks in the ITO electrode that form when the electrode undergoes sufficient strain.

conditions, the copper tape prevented the increase in resistance seen in the unmodified electrode (Figure 5A). However, one limitation of this approach is that the tape can only bridge cracks caused by bending in one direction. If bending occurs along more than one axis, cracking would cause the ITO

segments to be isolated from all sides of the electrode. A conductive bridge applied to the edge of the electrode would not be able to connect the segments in the middle of the film. To overcome this limitation, a conductive bridge needs to connect the entirety of the ITO electrode.

In the second approach, the electrodeposited material serves as the conductive bridge between isolated ITO segments. Because this bridge covers the whole electrode, this method could be used in the case of bending along multiple axes. Initially, we attempted to use PANI as the conductive bridge but found that the resistance was not improved (Supporting Information Figure S4). PEDOT:PSS, another flexible conductive polymer commonly used in photovoltaic devices,³ was electrochemically deposited onto ITO electrodes and explored as a bridge material. We found that the PEDOT:PSS film did provide an improved resistance at higher strain compared with the unmodified ITO electrode (Figure 5A).

The electrochemical performance of the modified electrodes was then evaluated using chronoamperometry in a ferri/ferrocyanide electrolyte (Figure 5B). Under flat, unstrained configurations, the anodic current at 30 s for modified and unmodified ITO electrodes was similar, demonstrating that the modifications have little to no impact on the electrochemical performance using a typical electrolyte. Under high-strain conditions, however, the current observed using an unmodified ITO electrode is drastically reduced. The PEDOT:PSS-modified electrodes unfortunately did not demonstrate significant improvement of the electrochemical activity under high-strain conditions relative to the unmodified ITO. This could be caused by the PEDOT:PSS not having a high enough conductivity to transfer electrons at a rate necessary for good chronoamperometry performance. The copper-tape-modified electrodes, however, demonstrated nearly identical performance in the high-strain and unstrained configurations. Durability experiments using this copper-tape modification found that the electrochemical activity of the electrode remained well above that of unmodified ITO electrodes even after 50 bending cycles (Figure S5). The ability for copper-tape modification to maintain the electrochemical activity of the ITO electrode was further exemplified through the electrodeposition of PANI at a normalized strain of 0.33 (bending radius of 3 mm). Without the copper tape as a bridge, deposition is incomplete as previously mentioned, due to cracks caused by bending (Figure 5C). When the copper-tape electrical bridge is applied, deposition occurs consistently across the width of the electrode (Figure 5D). Importantly, the copper tape must be applied to the electrode when flat to ensure good adhesion, and the copper must not contact the electrolyte to avoid the introduction of copper contaminants in the electrolyte solution. The application of copper tape provides a simple and effective method for overcoming the cracking in the ITO layer.

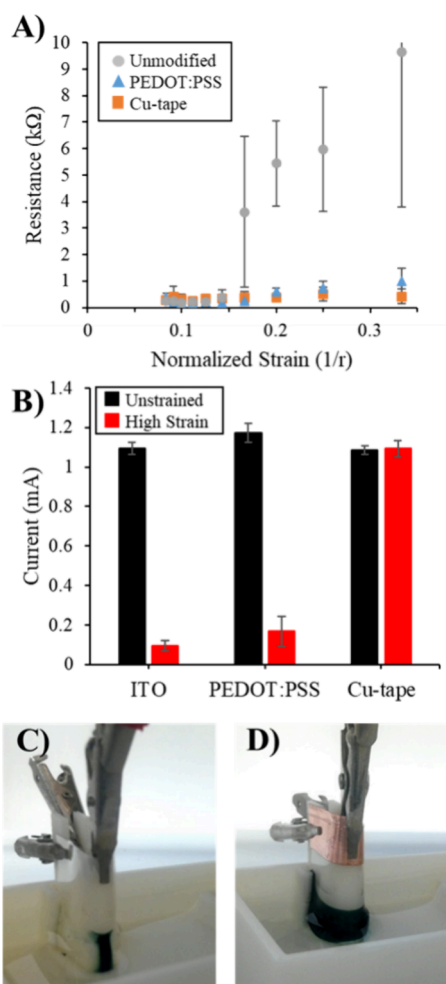


Figure 5. Effect of strain on modified ITO substrates. (A) Resistance measurements for PEDOT:PSS-modified (blue), and copper-tape-modified (orange) electrodes under different levels of strain ($1/\text{bending radius}$). Unmodified electrodes (gray) are included as a point of reference. Error bars represent the standard deviation from at least 3 unique samples. (B) Anodic current at 30 s during a chronoamperometry experiment in a ferri/ferrocyanide electrolyte under unstrained (black) and high-strain (red, 0.33 normalized strain) conditions. (C) Photograph of the nonuniform electrodeposition of PANI on an unmodified ITO electrode under high-strain conditions and (D) photograph of the uniform electrodeposition of PANI on a copper-tape-modified ITO electrode while under high-strain conditions during electrodeposition.

To illustrate the utility of this method, we performed electrochromic experiments on electrodeposited PANI films. PANI has received a lot of attention for its electrochromic abilities due to its low cost, environmental stability, and obvious color contrast between its bleached (reduced) and colored (oxidized) states.^{29–33} These applications include electrochromic windows,³⁴ electronic displays,³⁵ and antiglare mirrors.³⁶ In our experiments, we prepared PANI films on unmodified and copper-tape-modified ITO electrodes under flat conditions. The PANI films were then transferred to a 1 M H₂SO₄ electrolyte, and a -0.2V vs Ag/AgCl was applied for 30 s in order to reduce the PANI to its bleached state. When using copper-tape-modified electrodes, the change in NIR-visible absorbance of the PANI film under high-strain conditions (3 mm bending radius) was similar to that of unmodified ITO under unstrained conditions (Figure 6). Importantly, bleaching

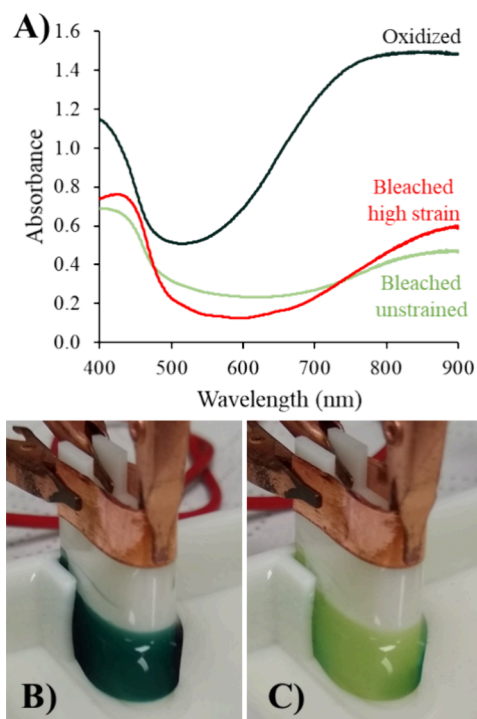


Figure 6. Electrochromic behavior of PANI on Cu-tape-modified ITO. (A) UV-vis spectra of as deposited oxidized PANI (black), bleached PANI under unstrained conditions (green), and bleached PANI under high-strain conditions (red, 3 mm bending radius). (B) Photographs of the oxidized PANI and (C) bleached PANI under high-strain conditions.

experiments of PANI on unmodified ITO at a 3 mm bending radius did not show a significant change in absorption, and only minimal reducing current was observed during these experiments (see Supporting Information Figure S6). This proof-of-concept experiment demonstrates how copper-tape modification can enhance the performance of ITO-PET-based electrodes under high-strain conditions.

CONCLUSIONS

The electrochemical performance of commercially available flexible ITO electrodes under strained conditions has been evaluated using the electrodeposition of PANI as a test system. Due to the brittle nature of ITO, bending to high-strain conditions results in the formation of cracks that are

detrimental to uniform electrochemical performance. For electrochemical applications, the use of thinner ITO layers to gain increased flexibility does not appear to be a viable solution due to the increased resistance of these thinner ITO films. The issue of ITO cracking can be overcome by using conductive materials to bridge the various segments of the ITO under crack-inducing strains. This was demonstrated using copper tape applied to the top of the electrode. The application of copper tape enabled much improved electrochemical performance under high-strain conditions without affecting the transparency of the electrochemically active region of the ITO electrode. This was demonstrated using the electrochromic bleaching of PANI at a low bending radius. This copper-tape modification strategy can be implemented to maintain electrical conductivity under a single-direction strain application such as flexible solar cells or electrochromic windows. For applications requiring flexibility along multiple axes, the isolated segments of the ITO would need to be connected using a flexible conductive film across the entire electrode. Our preliminary experiments using PEDOT:PSS demonstrated promising results in regard to resistance change, though other materials may need to be explored to enable desired electrochemical performance. With these findings, these inexpensive and versatile electrodes can be used in more applied electrochemical devices and studies that require flexibility and electrochemical functionality, such as wearable sensors,¹² flexible photovoltaics,² and roll-to-roll electro-deposition.³⁷

METHODS

Materials. All chemicals were used as received. Aniline was purchased from TCI America. Potassium ferrocyanide trihydrate and potassium ferricyanide were purchased from Fisher Scientific. Potassium chloride was purchased from VWR. 3,4-Ethylenedioxythiophene, 18 wt % in H₂O Poly(4-styrenesulfonic acid) solution (MW ~75,000), H₂SO₄, and ITO-PET substrates were purchased from Sigma Aldrich. A table listing the specific item numbers and characteristics of the ITO-PET substrates can be found in the Supporting Information (Table S1). ITO-PET samples were cut to size using a portable paper trimmer (Fiskars) which was important for avoiding the bending of the electrodes during the cutting process. Aqueous solutions were prepared using high-purity water (18 M Ω). Electrochemical cells were prepared using a 3D printer (Prusa MK3S or Lulzbot mini) with natural ABS filament from MatterHackers Inc. Additional information about the 3D printing parameters and how to access the digital designs for free can be found in the Supporting Information.

Resistance Testing. Electrical resistance measurements were performed using linear sweep voltammetry using a Biologic SAS SP300 Potentiostat. An electrical connection was made using microsteel or copper toothless alligator clips with a jaw opening of 5.6 mm (Uniquers). The length between electrical connections was 28 mm. The voltage was swept from -0.1 to $+0.1$ V at 10 mV/s. Resistance was calculated by dividing the change in voltage by the change in current. Resistance testing was performed in 3D-printed devices designed to hold the electrodes at specific bending radii. Reported measurements represent averages of at least 3 unique samples at each bending radius.

Electron Microscopy. After ITO specimens were subjected to bending, the specimens were examined for evidence

of cracking with a scanning electron microscope (FEI Helios NanoLab). Specimens were first sputter coated with a ~ 10 nm layer of gold/palladium to reduce charging due to the differing conductivities of PANI and ITO. The accelerating voltage used during imaging was 15.0 kV. During imaging, specimens were examined with a scanning pattern beginning in the center of the film and proceeding to either side to cover an area of up to 15 mm \times 15 mm. If crack images were captured, ImageJ was used to measure the distances between cracks.

Electrochemical Experiments. All electrochemical experiments were performed using a Biologic SAS SP300 Potentiostat. A Ag/AgCl electrode (CH Instruments) and a platinum electrode were used as the reference and counter electrodes, respectively. The ITO-PET electrode (30 mm \times 40 mm) was used as the working electrode and held at specific bending radii by the 3D-printed electrochemical cell and toothless alligator clips. An electrical connection was made to one of the toothless alligator clips. The electrolyte for PANI deposition consisted of 100 mM aniline in 1 M H₂SO₄. Electrodeposition of PANI was accomplished by applying 2.0 V vs Ag/AgCl until 0.2 mAh (0.72 C) had passed through the system. The electrolyte for the PEDOT:PSS deposition consisted of 10 mM 3,4-Ethylenedioxythiophene (EDOT) and 1% PSS (Poly 4-styrenesulfonic acid). As an example, 0.500 L of this aqueous electrolyte was prepared by mixing 534 μ L of EDOT and 25 mL of 18% PSS. Electrodeposition of the PEDOT:PSS film was accomplished by applying 1.5 V vs Ag/AgCl until 0.2 mAh (0.72 C) had passed through the system or a maximum of 5 min had elapsed. Typical deposition curves for both PANI and PEDOT:PSS can be seen in the Supporting Information (Figure S7). Using a constant charge resulted in a more reproducible film thickness than using a specific deposition time. Under ideal conditions (uniform deposition) the 0.2 mAh deposition took 50–80 s for PANI films and 110–160 s for PEDOT:PSS films. Following deposition, the films were dipped in high-purity water before further analysis. Chronoamperometry analysis was performed using a ferri/ferro-cyanide electrolyte consisting of 10 mM ferricyanide, 10 mM ferrocyanide, and 100 mM KCl. The anodic current at 30 s was used to evaluate the effects of strain on the electrodes. Average values were determined from at least 3 unique samples. Electrochromic analysis was performed by first electrodepositing PANI on unmodified or Cu-tape-modified ITO substrates under unstrained conditions. Films were then dipped in high-purity water before transferring to a 1 M H₂SO₄ electrolyte. A voltage of -0.2 V vs Ag/AgCl was applied to bleach the PANI films.

Photoanalysis of Film Deposition. The deposition area of the electrodeposited films was quantified using ImageJ, a public-domain Java image processing program. To determine the uniformity of the films (Figure 1), the “Plot Profile” tool was used on a line drawn from the top of the electrodeposited PANI film to the bottom of the electrode. The gray value was used to evaluate the darkness of the film, with a lower gray value representing a darker (thicker) film. To determine the area of each electrode that was coated in PANI (Figure 2), we employed a “Color Threshold” feature in ImageJ using a color intensity value of 75 to isolate the regions with significant film deposition.

UV–Vis Analysis. UV–vis spectra were performed using a Shimadzu UV-1800 spectrometer with a modification of the 3D-printed adapter described in previous work.³⁸

■ ASSOCIATED CONTENT

Supporting Information

The Supporting Information is available free of charge at <https://pubs.acs.org/doi/10.1021/acsomega.4c03288>.

Table of ITO substrates analyzed in this study; 3D printing information; effect of ITO resistance on the uniformity of PANI electrodeposition; effect of electrical contact point on high-strain electrodepositions; analysis of crack distance as a function of bending radius; resistance of PANI-modified ITO as a function of normalized strain; durability analysis of copper-tape modified ITO electrodes; chronoamperometry data for electrochromic experiments; and chronoamperometry data for typical electrodepositions (PDF)

■ AUTHOR INFORMATION

Corresponding Author

Gabriel LeBlanc – Chemistry and Biochemistry, University of Tulsa, Tulsa, Oklahoma 74104, United States; orcid.org/0000-0002-3331-9734; Email: gabriel-leblanc@utulsa.edu

Authors

Laura J. Waldman – Mechanical Engineering, University of Tulsa, Tulsa, Oklahoma 74104-9700, United States;

orcid.org/0000-0001-6598-7350

Daniel P. Haunert – Chemistry and Biochemistry, University of Tulsa, Tulsa, Oklahoma 74104, United States

Jack D. Carson – Chemistry and Biochemistry, University of Tulsa, Tulsa, Oklahoma 74104, United States

Nate Weiskopf – Chemistry and Biochemistry, University of Tulsa, Tulsa, Oklahoma 74104, United States

Julia V. Waldman – Chemistry and Biochemistry, University of Tulsa, Tulsa, Oklahoma 74104, United States

Complete contact information is available at: <https://pubs.acs.org/10.1021/acsomega.4c03288>

Notes

The authors declare no competing financial interest.

■ ACKNOWLEDGMENTS

This material is based upon work supported by the National Science Foundation under Grant No. 1852477. The authors also acknowledge financial support from The University of Tulsa, specifically the Office of Research and Sponsored Programs, the Tulsa Undergraduate Research Challenge Program, and the Chemistry Summer Undergraduate Research Program.

■ REFERENCES

- (1) Ouyang, C.; Liu, D.; He, K.; Kang, J. Recent Advances in Touch Sensors for Flexible Displays. *IEEE Open J. Nanotechnol.* **2022**, *4*, 36.
- (2) Brown, M. T.; Rossi, F. D.; Giacomo, F. D.; Mincuzzi, G.; Zardetto, V.; Reale, A.; Carlo, A. D. Progress in Flexible Dye Solar Cell Materials, Processes and Devices. *J. Mater. Chem. A* **2014**, *2* (28), 10788–10817.
- (3) Zardetto, V.; Brown, T. M.; Reale, A.; Di carlo, A. Substrates for Flexible Electronics: A Practical Investigation on the Electrical, Film Flexibility, Optical, Temperature, and Solvent Resistance Properties. *Journal of Polymer Science Part B: Polymer Physics* **2011**, *49* (9), 638–648.
- (4) Demirhan, Y.; Koseoglu, H.; Turkoglu, F.; Uyanik, Z.; Ozdemir, M.; Aygun, G.; Ozyuzer, L. The Controllable Deposition of Large

Area Roll-to-Roll Sputtered ITO Thin Films for Photovoltaic Applications. *Renewable Energy* **2020**, *146*, 1549–1559.

(5) Park, H. J.; Kim, J.; Won, J. H.; Choi, K. S.; Lim, Y. T.; Shin, J. S.; Park, J.-U. Tin-Doped Indium Oxide Films for Highly Flexible Transparent Conducting Electrodes. *Thin Solid Films* **2016**, *615*, 8–12.

(6) Lu, S.-K.; Huang, J.-T.; Lee, T.-H.; Wang, J.-J.; Liu, D.-S. Flexibility of the Indium Tin Oxide Transparent Conductive Film Deposited onto the Plastic Substrate. *Smart Science* **2014**, *2* (1), 7–12.

(7) Datta, R. S.; Syed, N.; Zavabeti, A.; Jannat, A.; Mohiuddin, M.; Rokunuzzaman, Md.; Yue zhang, B.; Rahman, Md. A.; Atkin, P.; Messalea, K. A.; Ghasemian, M. B.; Gaspera, E. D.; Bhattacharyya, S.; Fuhrer, M. S.; Russo, S. P.; Mcconville, C. F.; Esrafilzadeh, D.; Kalantar-zadeh, K.; Daeneke, T. Flexible Two-Dimensional Indium Tin Oxide Fabricated Using a Liquid Metal Printing Technique. *Nature Electronics* **2020**, *3* (1), 51–58.

(8) Park, J. Y.; Park, H. J. Optoelectric Property and Flexibility of Tin-Doped Indium Oxide (ITO) Thin Film. *Journal of nanoscience and nanotechnology* **2020**, *20* (6), 3542–3546.

(9) Mitsubayashi, K.; Wakabayashi, Y.; Tanimoto, S.; Murotomi, D.; Endo, T. Optical-Transparent and Flexible Glucose Sensor with ITO Electrode. *Biosensors and Bioelectronics* **2003**, *19* (1), 67–71.

(10) Lo, M.; Diaw, A. K. D.; Gningue-sall, D.; Aaron, J.-J.; Oturan, M. A.; Chehimi, M. M. Tracking Metal Ions with Polypyrrole Thin Films Adhesively Bonded to Diazonium-Modified Flexible ITO Electrodes. *Environmental Science and Pollution Research* **2018**, *25* (20), 20012–20022.

(11) Bharatula, L. D.; Marsili, E.; Kwan, J. J. Impedimetric Detection of Pseudomonas Aeruginosa Attachment on Flexible ITO-Coated Polyethylene Terephthalate Substrates. *Electrochim. Acta* **2020**, *332*, No. 135390.

(12) Mazzara, F.; Patella, B.; D'agostino, C.; Bruno, M. G.; Carbone, S.; Lopresti, F.; Aiello, G.; Torino, C.; Vilasi, A.; O'riordan, A.; Inguanta, R. PANI-Based Wearable Electrochemical Sensor for pH Sweat Monitoring. *Chemosensors* **2021**, *9* (7), 169.

(13) Li, Y.; Wei, H.; Chen, Y.; Ma, J.; Zhang-peng, X.; Li, W.; Hu, F. A Novel Flexible Electrochemical Molecular Imprinted Sensor for the Determination of GABA in Serum of Depressed Mice. *J. Electrochem. Soc.* **2023**, *170* (1), No. 017504.

(14) Tripathy, S.; Joseph, J.; Vanjari, S. R. K.; Rao, A. N.; Singh, S. G. Flexible ITO Electrode With Gold Nanostructures for Femtomolar DNA Hybridization Detection. *IEEE sensors letters* **2018**, *2* (4), 1–4.

(15) Siopa, D.; Gomes, A. Nucleation and Growth of ZnO Nanorod Arrays onto Flexible Substrates. *J. Electrochem. Soc.* **2013**, *160* (10), D476.

(16) Ebrahimi, H.; Yaghoubi, H.; Giammattei, F.; Takshi, A. Electrochemical Detection of Piezoelectric Effect from Misaligned Zinc Oxide Nanowires Grown on a Flexible Electrode. *Electrochim. Acta* **2014**, *134*, 435–441.

(17) Samanta, S.; Bakas, I.; Singh, A.; Aswal, D. K.; Chehimi, M. M. In Situ Diazonium-Modified Flexible ITO-Coated PEN Substrates for the Deposition of Adherent Silver–Polypyrrole Nanocomposite Films. *Langmuir* **2014**, *30* (31), 9397–9406.

(18) Perry, S. C.; Arumugam, S.; Beeby, S.; Nandhakumar, I. Template-Free Nanostructured Poly-3-Hexylthiophene (P3HT) Films via Single Pulse-Nucleated Electrodeposition. *J. Electroanal. Chem.* **2023**, *933*, No. 117278.

(19) Sajadpour, M.; Siampour, H.; Abbasian, S.; Amiri, M.; Rameshan, R.; Rameshan, C.; Hajian, A.; Bagheri, H.; Moshaii, A. A Non-Enzymatic Glucose Sensor Based on the Hybrid Thin Films of Cu on Acetanilide/ITO. *J. Electrochem. Soc.* **2019**, *166* (13), B1116.

(20) Nagaraju, G.; Ko, Y. H.; Yu, J. S. Effect of Diameter and Height of Electrochemically-Deposited ZnO Nanorod Arrays on the Performance of Piezoelectric Nanogenerators. *Mater. Chem. Phys.* **2015**, *149–150*, 393–399.

(21) Zhou, D.; Che, B.; Lu, X. Rapid One-Pot Electrodeposition of Polyaniline/Manganese Dioxide Hybrids: A Facile Approach to Stable

High-Performance Anodic Electrochromic Materials. *Journal of Materials Chemistry C* **2017**, *5* (7), 1758–1766.

(22) Kim, J.; Sohn, J.; Jo, Y.; Woo, H.; Han, J.; Cho, S.; Inamdar, A. I.; Kim, H.; Im, H. Drop-Casted Polyaniline Thin Films on Flexible Substrates for Supercapacitor Applications. *Journal of the Korean Physical Society* **2014**, *65* (9), 1320–1323.

(23) Guo, Y.; Li, W.; Yu, H.; Perepichka, D. F.; Meng, H. Flexible Asymmetric Supercapacitors via Spray Coating of a New Electrochromic Donor–Acceptor Polymer. *Advanced Energy Materials* **2017**, *7* (2), 1601623.

(24) Wirth, D. M.; Waldman, L. J.; Petty, M.; Leblanc, G. Communication—Polyaniline Electrodeposition on Flexible ITO Substrates and the Effect of Curved Electrochemical Conditions. *Journal of The Electrochemical Society* **2019**, *166* (13), D635–D637.

(25) Armini, S.; Vereecken, P. M. Impact of “Terminal Effect” on Cu Plating: Theory and Experimental Evidence. *ECS Trans.* **2010**, *25* (27), 185.

(26) Ho, K.-C.; Singleton, D. E.; Greenberg, C. B. The Influence of Terminal Effect on the Performance of Electrochromic Windows. *J. Electrochem. Soc.* **1990**, *137* (12), 3858.

(27) Qu, J.; Garabedian, N.; Burris, D. L.; Martin, D. C. Durability of Poly(3,4-Ethylenedioxythiophene) (PEDOT) Films on Metallic Substrates for Bioelectronics and the Dominant Role of Relative Shear Strength. *Journal of the Mechanical Behavior of Biomedical Materials* **2019**, *100*, No. 103376.

(28) Qu, J.; Ouyang, L.; Kuo, C.; Martin, D. C. Stiffness, Strength and Adhesion Characterization of Electrochemically Deposited Conjugated Polymer Films. *Acta Biomaterialia* **2016**, *31*, 114–121.

(29) Nguyen, T. V.; Le, Q. V.; Peng, S.; Dai, Z.; Ahn, S. H.; Kim, S. Y. Exploring Conducting Polymers as a Promising Alternative for Electrochromic Devices. *Advanced Materials Technologies* **2023**, *8* (18), 2300474.

(30) Beygisangchin, M.; Abdul rashid, S.; Shafie, S.; Sadrollhosseini, A. R.; Lim, H. N. Preparations, Properties, and Applications of Polyaniline and Polyaniline Thin Films—A Review. *Polymers* **2021**, *13* (12), 2003.

(31) Rai, V.; Singh, R. S.; Blackwood, D. J.; Zhili, D. A Review on Recent Advances in Electrochromic Devices: A Material Approach. *Advanced Engineering Materials* **2020**, *22* (8), 2000082.

(32) Zhao, L.; Zhao, L.; Xu, Y.; Qiu, T.; Zhi, L.; Shi, G. Polyaniline Electrochromic Devices with Transparent Graphene Electrodes. *Electrochim. Acta* **2009**, *55* (2), 491–497.

(33) Sare, H.; Dong, D. Electrochromic Polymers: From Electrodeposition to Hybrid Solid Devices. *Energies* **2024**, *17* (1), 232.

(34) Yilmaz, P.; Magni, M.; Martinez, S.; Gonzalez gil, R. M.; Della pirriera, M.; Manca, M. Spectrally Selective PANI/ITO Nanocomposite Electrodes for Energy-Efficient Dual Band Electrochromic Windows. *ACS Appl. Energy Mater.* **2020**, *3* (4), 3779–3788.

(35) Zhang, S.; Ren, J.; Chen, S.; Luo, Y.; Bai, X.; Ye, L.; Yang, F.; Cao, Y. Large Area Electrochromic Displays with Ultrafast Response Speed and High Contrast Using Solution-Processable and Patternable Honeycomb-like Polyaniline Nanostructures. *J. Electroanal. Chem.* **2020**, *870*, No. 114248.

(36) Brasse, Y.; Ng, C.; Magnozzi, M.; Zhang, H.; Mulvaney, P.; Fery, A.; Gómez, D. E. A Tunable Polymer–Metal Based Anti-Reflective Metasurface. *Macromol. Rapid Commun.* **2020**, *41* (1), 1900415.

(37) Huang, Y.; Yang, C.; Lang, J.; Zhang, S.; Feng, S.; Schaefer, L.-A.; Carney, T. J.; Mu, J.; Lin, S.; Zhou, Y.; Long, Y.; Kong, D.; Li, Q.; Li, X.; Wu, H. Metal Nanoparticle Harvesting by Continuous Rotating Electrodeposition and Separation. *Matter* **2020**, *3* (4), 1294–1307.

(38) Whitehead, H. D.; Waldman, J. V.; Wirth, D. M.; Leblanc, G. 3D Printed UV–Visible Cuvette Adapter for Low-Cost and Versatile Spectroscopic Experiments. *ACS Omega* **2017**, *2* (9), 6118–6122.